



Univerzita Komenského v Bratislave  
Fakulta matematiky, fyziky a informatiky



**Mgr. Juraj Beňo**

Autoreferát dizertačnej práce

## **Simulations of cosmogenic radionuclide production rates in meteorites and Earth's atmosphere**

**na získanie akademického titulu philosophiae doctor**

v odbore doktorandského štúdia:

4.1.5 Jadrová a subjadrová fyzika

Bratislava 2014

Dizertačná práca bola vypracovaná v dennej forme doktorandského štúdia na Katedre jadrovej fyziky a biofyziky

**Predkladateľ:**           **Mgr. Juraj Beňo**  
Katedra jadrovej fyziky a biofyziky  
Fakulta matematiky, fyziky a informatiky  
Univerzita Komenského  
842 48 Bratislava 4

**Školiteľ:**                   **prof. RNDr. Jozef Masarik, DrCs.**

**Oponenti:**               **1.**  
  
**2.**  
  
**3.**

**Obhajoba dizertačnej práce sa koná ..... o ..... h  
pred komisiou pre obhajobu dizertačnej práce v odbore doktorandského štúdia  
vymenovanou predsedom odborovej komisie .....**

Štúdijný odbor:           4.1.5 Jadrová a subjadrová fyzika,  
Štúdijný program:       Jadrová a subjadrová fyzika.

na Fakulte matematiky, fyziky a informatiky Univerzity Komenského, Mlynská dolina, 842  
48 Bratislava, miestnosť .....

**Predseda odborovej komisie:**

**prof. RNDr. Jozef Masarik, DrCs.**  
Katedra jadrovej fyziky a biofyziky  
FMFI UK, 842 48 Bratislava

# Table of Contents

Introduction .....	4
Aims .....	4
Effect of pre-atmospheric shape on cosmogenic nuclide production.....	5
Simulations .....	5
Results and discussion .....	6
Calculation model for short-lived cosmogenic radionuclides .....	9
Calculation model.....	9
Results.....	12
Discussion.....	13
The Chelyabinsk meteorite and The Košice meteorite.....	14
Simulations .....	15
Results and discussion .....	16
Atmospheric <sup>81</sup> Kr as an integrator of cosmic-ray flux over the past 800 kyr.....	18
Results and discussion .....	19
A model for the production rate of <sup>81</sup> Kr .....	20
Summary.....	21
Publications .....	23

## Introduction

This work was dedicated to the Monte-Carlo modelling of cosmic ray interactions with extra-terrestrial and terrestrial matter. A large variety of stable and radioactive cosmogenic nuclides is produced by interaction of cosmic ray particles with matter. The investigation of these cosmogenic nuclides allows us to study the history of the irradiated bodies in the solar system as well as that of the cosmic radiation itself. For interpretation of measured abundances of cosmogenic nuclides a precise and accurate modelling of the depth and size dependence of cosmic ray interactions in target body is necessary. This work discusses results achieved using calculation models oriented on production of cosmogenic radionuclides commonly used in applied nuclear physics.

## Aims

The main tasks of the dissertation are:

- Study of cosmogenic nuclide production rates dependence on the preatmospheric shape of irradiated body.
- Investigation of solar activity on short lived cosmogenic nuclide production by galactic cosmic rays.
- Modelling of production rates for Košice and Chelyabinsk meteorites.
- Simulation of  $^{81}\text{Kr}$  production in the Earth's atmosphere.

## **Effect of pre-atmospheric shape on cosmogenic nuclide production**

Productions rates of cosmogenic nuclides are dependent on few major factors such as: incident particle fluxes, the meteoroid's preatmospheric shape and size, and its bulk chemical composition. Size effects [1] and bulk chemical composition effects [2] have been studied in details in the past years. Therefore we concentrate our attention in this chapter on effects of the parent body shape.

### **Simulations**

Our calculations were carried out for a meteorite with composition of an average L chondrite, which belong to the most frequent meteorite types. Sizes of investigated spherical meteoroids were 90 and 180 cm in diameter. Such range of diameters covers the most typical sizes of meteoroids and allowed us to investigate potential changes in shape effects related to the various sizes of meteoroids. Volumes and masses of modelled object with different geometries were equal. This allowed us to distinguish size and shape effects in final data.

The Peekskill meteorite used for comparison of experimental data with simulation has fallen on 9<sup>th</sup> October 1992 in Peekskill, New York [3]. The fall of the meteorite was observed and recorded by many observers. Object was fragmented into over 70 pieces. Analysis of meteorite fragments classified the Peekskill meteorite as H6 chondrite [3]. Based on dynamic data of the observed fireball a flattened geometry for the Peekskill meteoroid has been suggested [4]. Also measured activities of cosmogenic radionuclides, especially <sup>60</sup>Co, suggest either multistage exposure of the meteorite or flattened geometry [3].

The nucleon spectra were calculated by using the LCS [10] and MCNP. All investigated spheres, ellipsoids and cylinders had equal volumes. Particle fluxes for sphere were averaged through the whole surface of the every shell. In the cases of ellipsoids and cylinders fluxes were calculated for the small areas created by interception of particular surface and small cylinder with radius 2.5 cm crossing the modeled body. This approach allowed to calculate particle fluxes and production rate of radionuclides in vicinity of major axis of a particular geometry.

All simulated geometries were irradiated by averaged GCR flux  $\Phi = 550$  MeV and energy integrated primary cosmic ray particle flux  $4.8 \text{ part. cm}^{-2} \text{ s}^{-1}$ .

## Results and discussion

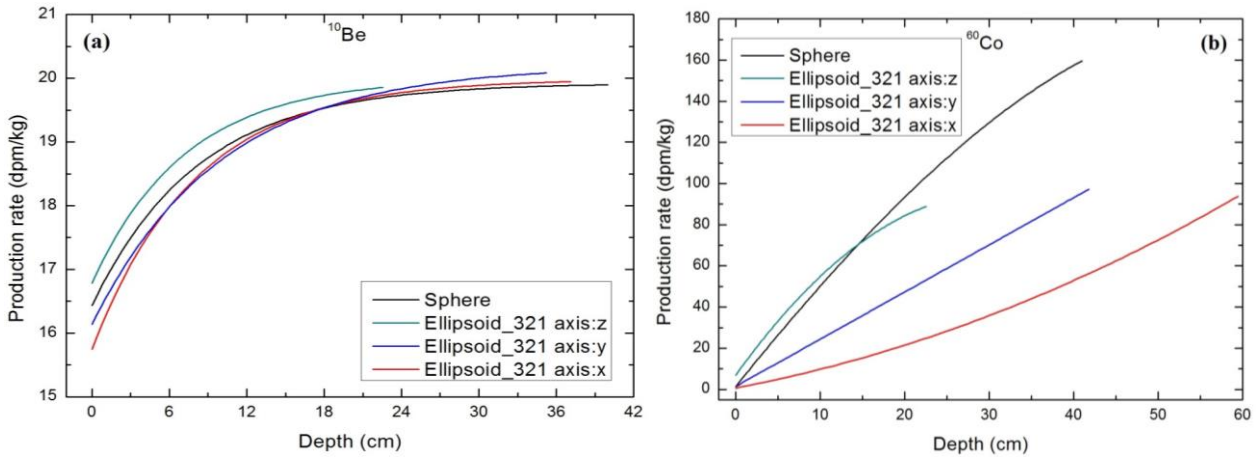


**Figure 1:** Depth profile for ellipsoidal geometry with semi-axes ratio 3:2:1 (x:y:z) in comparison with spherical geometry ( $R = 45$  cm)

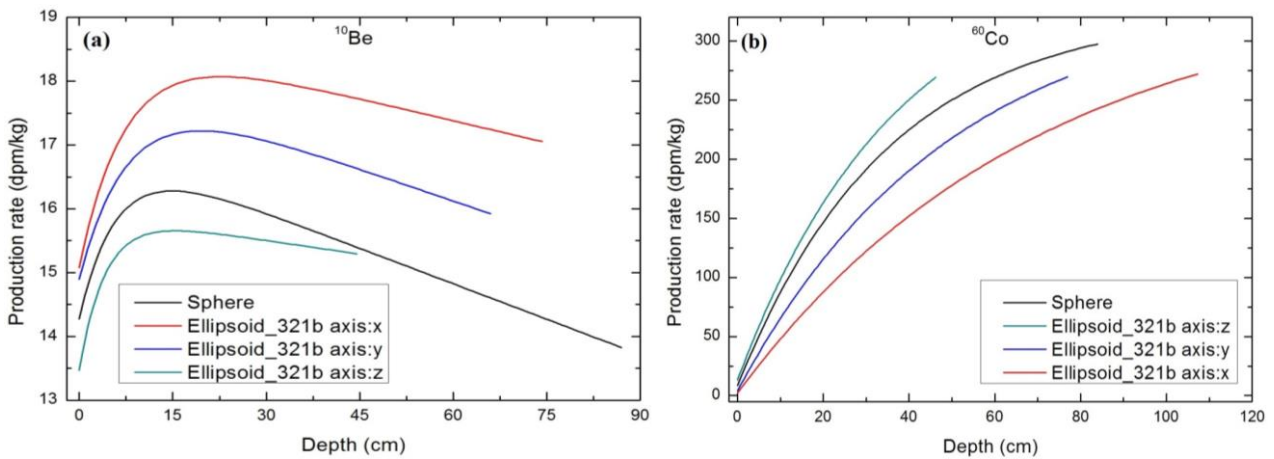


**Figure 2:** Depth profile for ellipsoidal geometry with semi-axes ratio 3:2:1 (x:y:z) in comparison with spherical geometry ( $R = 90$  cm)

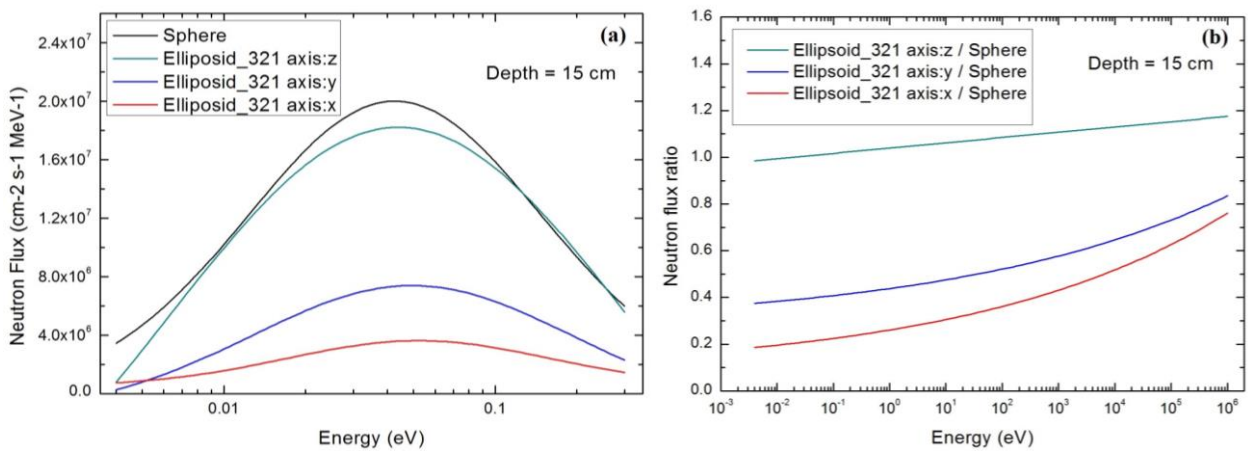


**Figure 3:** a, Comparison of the low-energy neutron fluxes in vicinity of semi axes of ellipsoid and sphere at depth of 15 cm.  
b, Ratio of neutron fluxes in ellipsoid to neutron flux in sphere at depth of 15 cm

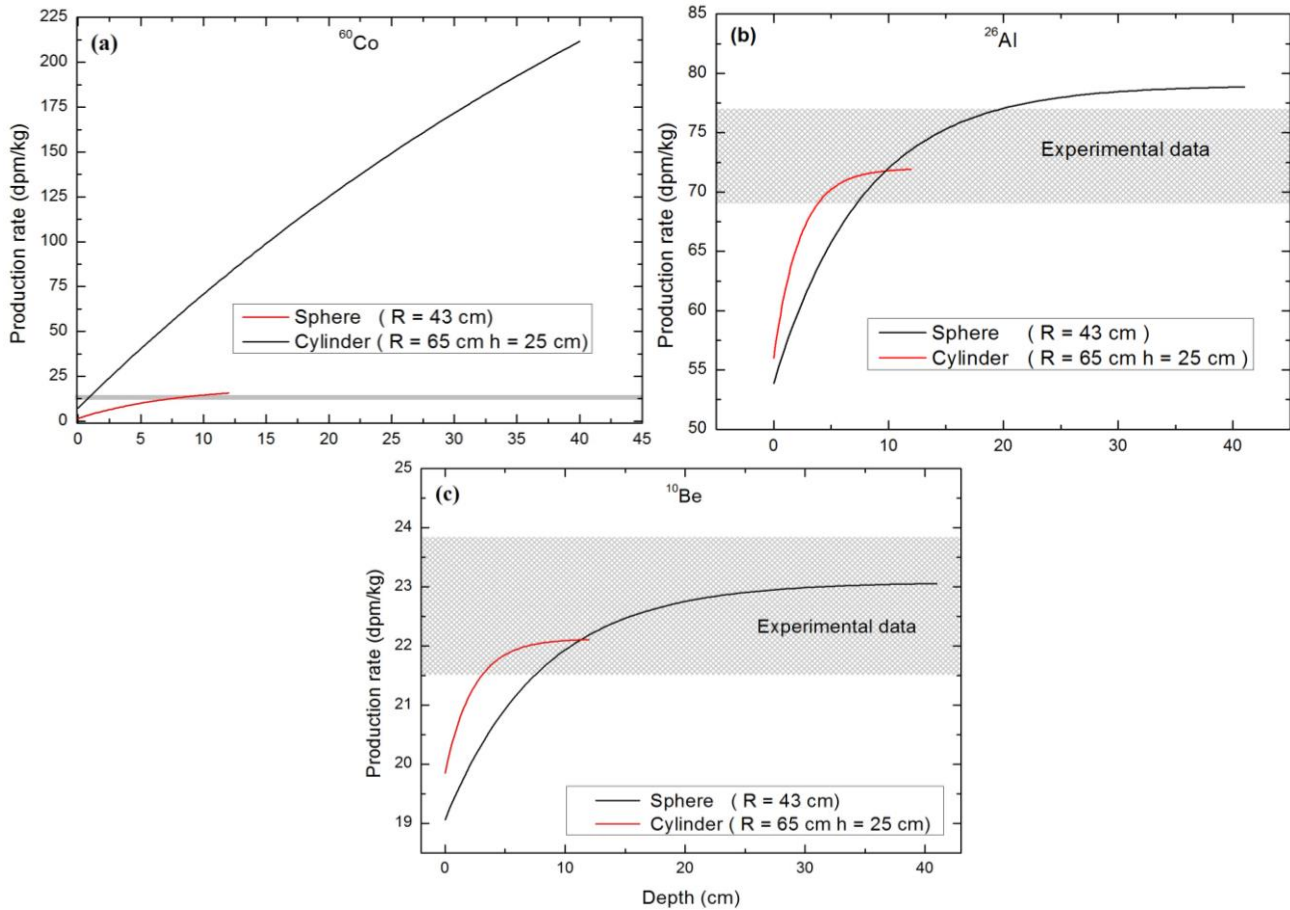


**Figure 4:** Depth profiles of  $^{60}\text{Co}$ ,  $^{26}\text{Al}$ ,  $^{10}\text{Be}$  in the Peekskill meteorite for cylindrical and spherical geometry in comparison with range of measured experimental data (grey).

The LCS/HMCP code has been used for an investigation of effect of preatmospheric shape on production rates of cosmogenic radionuclides. The cosmogenic radionuclides calculated are  $^{10}\text{Be}$  (as a product of high-energy spallation reactions) and  $^{60}\text{Co}$  (as a product of low-energy neutron capture). As one can see from figures 1a for the meter-sized meteoroid production rates for  $^{10}\text{Be}$  are insensitive to shape of the preatmospheric body as the simulated depth profile for all axes of all geometries are almost identical and small differences in calculated depth profiles are rather issue related to statistic. The production rates of  $^{60}\text{Co}$  are significantly different from those of  $^{10}\text{Be}$ . Figures 1b shows that production rate of  $^{60}\text{Co}$  vary significantly and this variation is related to the deformation of an object. For the same depth within the meteoroid's body but for the different axis very different production rate is obtained. Further, all depth profiles converge to the same value (in the center of meteoroid) but this value is lowered in comparison with maximal value obtained in the case spherical geometry. This is not the case for the a cylindrical geometry with length to radius ratio 2:1, which means that

bulk of this object is similar to sphere with rather deformed surface ( the length of the main object's axes are the same). Calculated depth profiles of  $^{10}\text{Be}$  and  $^{60}\text{Co}$  lead to the conclusion that the shape of the preatmospheric body rather influences particles of lower energies than those of higher energies. This effect is demonstrated on figure 3a,b, where figure a, shows differences in the fluxes for simulated ellipsoidal geometry in a short energy interval and figure b, shows ratios of fluxes on semiaxes of ellipsoid to fluxes in sphere which are obviously differ for lower energies and tend to converge with increasing energy. This investigation clarifies calculated depth profiles and theirs features. Explanation for observed effects is based on number of particles which escape from investigated body. Particle entering the body of meteoroid is involved in series of reactions and create many secondary particles. During this process particles either lose their energy or are absorbed. Considering shown examples we can say that the more is axis of an object elongated (and other shortened in comparison with spherical equivalent) in one direction the more is particle flux lowered due to reduced length for cascade development. This effect explain difference between particle fluxes and production rates in vicinity of axes of modeled bodies and also reduced maximal value reached in center of the objects in comparison to value reached in sphere.

Considering ~2 meter-sized geometries (Figures 2a,b) one can see different depth profiles form those for ~1 meter-sized geometries. This is due to the additional effect related to the size of modeled bodies. In the case of  $^{60}\text{Co}$  (Figure 2b) similar results are reached but differences among production rates on axes are lowered and also maximal value in comparison to sphere is similar. This is due to the additional space for cascade development added by enlarging the size of meteoroid resulting into slight compensation of differences in depth profiles. The depth profiles of  $^{10}\text{Be}$  (Figure 2a) show not only remarkable differences in production rate for the same depth but also inverted effect, where production rate is reduced on shortest axis (and sphere) and increased on longer axes at the same depth. The shape of depth profile curves is rising to about 15-20 cm of depth then follows slow decrease. This behavior is related to size of modeled object and flux intensity of high-energy secondary particles. Flux is rising due to very high energy of primary particles, which induce cascades of particles of lower energy until they reach energy at which corresponding excitation function for  $^{10}\text{Be}$  production reaches its maximum, but decrease of energy continues after that and naturally also production rate of  $^{10}\text{Be}$  starts decreasing with depth. In conclusion flattening renders the interior of the meteoroid to more accessible by high-energy particles, while increasing leakage of particles with lower energies.



The Peekskill meteorite was modeled as H chondrite with specific composition and with the proposed flattened geometry [3]. The modeled geometry was cylindrical with radius 65 cm and height of 25 cm and spherical geometry was modeled with radius 43 cm. The results of simulations shown on figures 3a,b,c show sufficient agreement for both proposed geometries in the case of  $^{10}\text{Be}$  and possibly also for  $^{26}\text{Al}$  (Figures 3b,c). The comparison of depth profiles of  $^{60}\text{Co}$  for spherical and cylindrical geometry yet shows large differences and measured experimental data are in better agreement with cylindrical geometry. This is caused by number of particles escaping from particular geometry (as it was already described in previous section). In the case of the cylindrical geometry, the contribution to the production rate is low due to small base to center distance and low effective cascade development from lateral side of the cylinder. The precise determination of the pre-atmospheric shape of a meteorite is not really possible due to very deformed shapes of real meteoroids, however approximation used in our work suggest possible explanation of measured data.

## Calculation model for short-lived cosmogenic radionuclides

The Sun and solar activity notably affects processes in heliosphere through generation of a perturbing heliospheric magnetic field. Those changes influence intensity of GCR flux in solar system mainly during eleven-year Schwabe cycle and the 22-year solar magnetic polarity cycle (other cycles are less pronounced). Variation in solar activity can induce only negligible effects on production of long-lived cosmogenic radionuclides such as  $^{26}\text{Al}$  ( $T_{1/2} = 7.17 \times 10^5$  y). In the case of short-lived cosmogenic radionuclides situation can't be described and solved as simple as in the case of long-lived cosmogenic radionuclides due to large variation in GCR particle fluxes over the solar cycle.

### Calculation model

Our effort here is to find the way to calculate production of a radionuclide with short half-life with consideration of temporal variation in source of radiation.

$$\frac{dN}{dt} = -\lambda N(t) + P_r(t) \quad (1)$$

And we were looking for exact formula for production rate  $P_r(t)$ .

The general equation which describes differential cosmic ray flux  $J_T(E, \Phi)$  at Earth's orbit can be written as:

$$J_T(E, \Phi) = J_{LIS}(E + \Phi) \frac{E(E + 2E_0)}{(E + \Phi)(E + \Phi + 2E_0)} \quad (2)$$

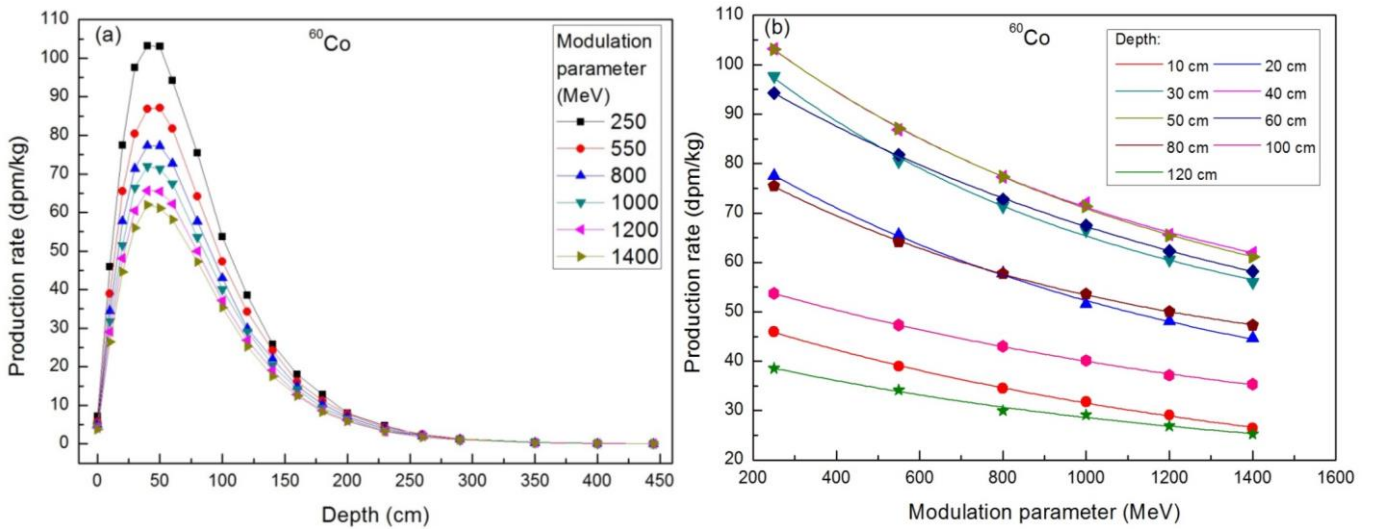
where  $E$  is kinetic energy,  $E_0$  is rest mass energy,  $\Phi$  is the modulation parameter and  $J_{LIS}(E + \Phi)$  represents unmodulated differential cosmic ray spectra (LIS). Second term describes modulation of cosmic ray flux.

LIS estimation by Usoskin [5].

$$J_{LIS}(E + \Phi) = \frac{1.9 \cdot 10^4 P(E)^{-2.78}}{1 + 0.4866 P(E)^{-2.51}} \quad (3)$$

where  $P(E) = \sqrt{E(E + 2E_0)}$   $E$  and  $J$  are expressed in units of [particles/(sr m<sup>2</sup> s GeV/nucleon)] and GeV/nucleon, respectively.

Using equation (2,3) we were able to obtain GCR spectrum and effective coefficients for various modulation parameters.



**Figures 5:** (a) - depth profile of <sup>60</sup>Co for various values of modulation parameter.

(b) - production rate in the specific depths as a function of modulation parameter fitted by exponential

$$\text{function: } a e^{b\Phi(t)} + e.$$

As we can see from shown example (Figures 5) all calculated dependences of production rate for particular radionuclide in specific depth on modulation parameter can be fitted well by simple exponential function  $f = a e^{b\Phi(t)} + e$ . Fit of experimental data with this function is

sufficient for every simulated meteorite of various sizes, composition and for every particular depth and radionuclide (despite decreasing tendency with depth). With this consideration equation 1 can be adjusted to:

$$\frac{dN}{dt} = -\lambda N(t) + ae^{b\Phi(t)} + e \quad (4)$$

Further use of equation 4 requires knowledge of changes of modulation parameter  $\Phi(t)$  over the periods of solar cycle. The Data required for this purpose are measured by neutron monitors and are consequently evaluated in order to obtain dependence on modulation parameter  $\Phi$  [5,7].

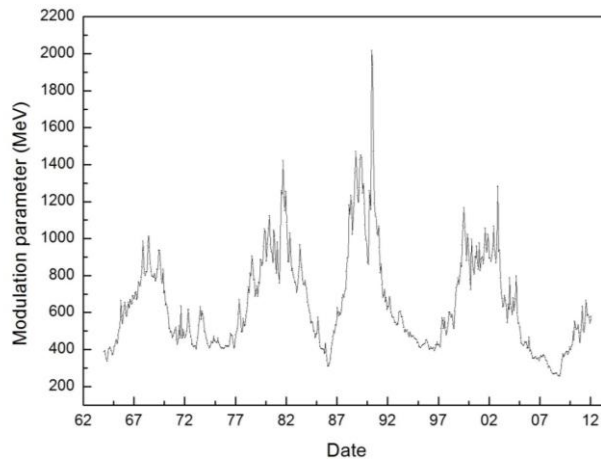


**Figure 6:** Time profile of reconstructed modulation parameter  $\phi$ . Mean 68% uncertainties are 140 MeV for July 1936 to January 1951; 44 MeV for February 1951 to March 1964; 26 MeV since April 1964. [5][7].

Based on fact that  $\Phi(t)$  function data are measured on daily basis  $\Phi(t)$  function can be split into small parts (days or months) which provide 3960 or 132 points per 11-years long cycle and one can use linear approximation among measured data and adjust equation 4 to the form:

$$\frac{dN}{dt} = -\lambda N(t) + ae^{b(ct+d)} + e \quad (5)$$

where  $N(t)$  - number of particular radionuclides,  $\lambda$  - decay constant of particular radionuclide, coefficients  $a, b, e$  come from fit of exponential function across the chosen  $\Phi$  parameters and coefficients  $c$  and  $d$  come from linear approximation of  $\Phi$  function between chosen time intervals ( days, months).

Solution of equation 5 for activity:

$$A(t) = e(1 - e^{-\lambda t}) + \frac{\lambda a e^{bd}}{bc + \lambda} (e^{bct} - e^{-\lambda t}) + A_0 e^{-\lambda t} \quad (6)$$

The equation 6 describes activity of a radionuclide at specific depth within a meteorite in a small time interval (day, month). The Equation takes into account production influenced by variable source of radiation (using linear change in a very small time interval) and natural decay of certain radionuclide. Term  $A_0$  represent activity at the beginning of the time interval and equation is recursive, so it should be applied multiple times in the way that  $A(t)$  from previous time interval is used as  $A_0$  in subsequent time period. This approach allows us to precisely calculate activity of particular radionuclide over a long time period (limited by the experimental data). Thus provides a way to reconstruct changes of activity of a particular radionuclide influenced by solar activity in long time before the fall of the meteorite.

## Results

We have applied approach described in previous section on known meteorites falls Chelyabinsk and Košice and we have reconstructed production of short-lived radionuclides in those meteorites many years back from a moment of the fall (7). The function of modulation parameter used in this calculation is evaluated for distance of 1 AU from the Sun and therefore activities of cosmogenic radionuclides are calculated for meteorites orbiting at 1 AU.

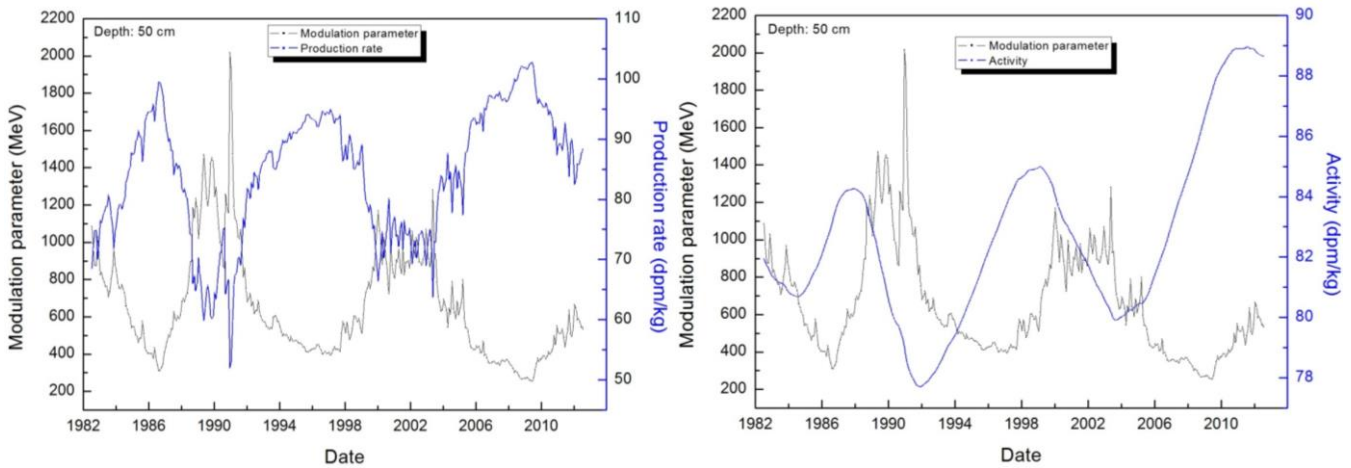


**Figure 7:** Reconstructed production rate (Up) and activity (Down) of  $^{60}\text{Co}$  (5.27 y) in the Chelyabinsk meteorite for a chosen depth. Calculated data are shown together with function of modulation parameter.

For the approximate evaluation of relative changes in production of cosmogenic radionuclide simple formula has been used:

$$A_{\Delta} = \frac{A_{(max)} - A_{(min)}}{A_{(min)}} * 100\% \quad (7)$$

Where  $A_{(max)}$  and  $A_{(min)}$  represents maximal and minimal calculated activity of specific radionuclide in a meteorite during solar cycle.

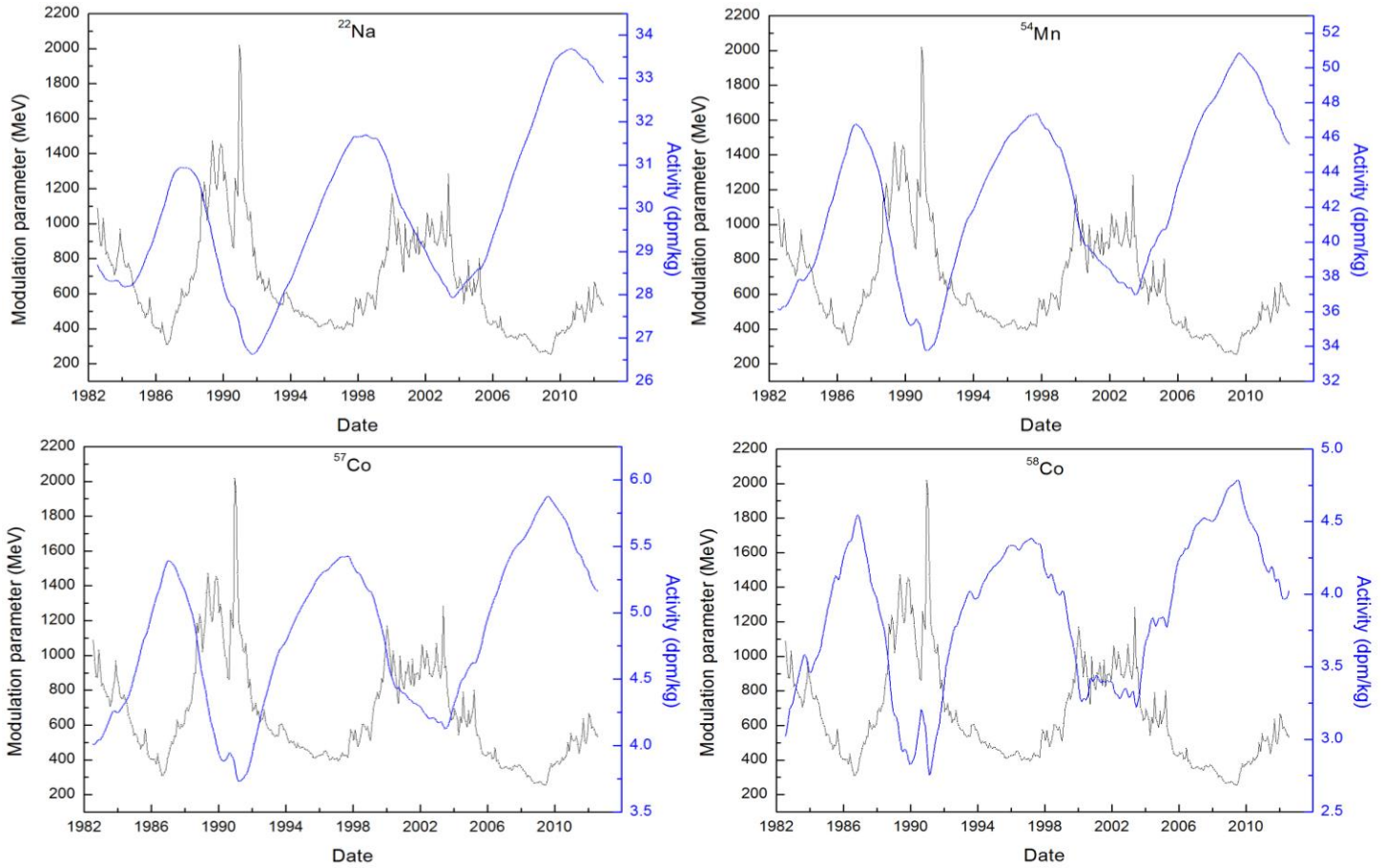


**Figure 8:** Reconstructed activities of  $^{22}\text{Na}$  (2.6 y),  $^{54}\text{Mn}$  (312.3 d),  $^{57}\text{Co}$  (271.8 d),  $^{58}\text{Co}$  (70.86 d) in the Chelyabinsk meteorite for a depth of 40 cm. Calculated data are shown together with function of modulation parameter.

## Discussion

The calculation model for short-lived radionuclides described in this chapter allowed us to reconstruct production rates and activities of cosmogenic radionuclides for known meteorite falls. Production rate of cosmogenic radionuclide is immediate response to changes in GCR as it is directly dependent on the source of irradiation, while activity rather integrates those

changes over time (figure 7). As one can see from figures 7,8 variations in activity of particular radionuclide (in this case between solar maximum and minimum) are dependent on its half-life, radionuclides with longer half-lives ~ few years undergo much lower variation (from equation 7); ~ 14 % for  $^{60}\text{Co}$  (5.27 y), ~ 26 % for  $^{22}\text{Na}$  (2.6 y) and radionuclide with shorter half-lives ~ tens or few hundred days are influenced much more by current solar activity and therefore we can see very strong variation in their activity; ~ 50 % for  $^{54}\text{Mn}$  (312.3 d), ~ 55 % for  $^{57}\text{Co}$  (271.8 d), ~ 70 % for  $^{58}\text{Co}$  (70.86 d) (7,8). The shape of simulated curves is somehow smoother and the position of local extreme is slightly shifted with increasing half-life. Those effects are due to aggregation and decay of radionuclides through the longer period of time, because radionuclides with longer half-lives are less sensitive on changes in GCR flux and their response to change is weaker and slightly delayed. Radionuclides with half-life much longer than 11y solar cycle period average out changes in solar activity and they are rather influenced by averaged GCR spectrum. As it was described in previous chapter, solar modulation strongly influence particles with lower energies and this influence lose strength with increasing energy, therefore variation in activity of a radionuclide is also naturally higher near surface, where many lower energetic particles contribute to production, and decreases with depth (5).

Described results clarify behaviour of short-lived nuclides through the solar cycle and have direct impact on their application e.g. the preatmospheric size of a meteoroid that is commonly estimated from activity of  $^{60}\text{Co}$  ( $^{60}\text{Co}$  is the one of the most sensitive depth indicators [8]). Its activity is calculated either from averaged GCR flux or using a very rough approximation of the solar activity. Precisely calculated activities of short-lived radionuclides can become useful tool for accurate estimation of depth of a particular sample in meteorite body and can provide very helpful information about characteristics of investigated meteorite.

## **The Chelyabinsk meteorite and The Košice meteorite**

The meteorite falls provide useful information for the study of the interaction of cosmic rays with matter, evolution of the solar system and meteorites itself. This information is obtained from analysis of meteorite fragments. Many fragments from falls of the Chelyabinsk and the Košice meteorite were analysed. We have used experimental data from both meteorites and calculated production rates and activities of measured cosmogenic radionuclides.

## Simulations

The Calculations of activities in the Chelyabinsk and the Košice meteorite were carried out by LCS [10]. Interaction of high energy particles ( $>20$  MeV) were calculated by lahet, low energy interactions ( $<20$ MeV) were calculated with hmcnp4. For calculations of activities in two approaches were used. First approach uses standard calculation model for long-lived cosmogenic nuclides (in our case  $^{26}\text{Al}$ ), where body of the meteorite is irradiated by averaged GCR flux  $\Phi = 550$  and integral flux  $4.8 \text{ nucleons cm}^{-2} \text{ s}^{-1}$  [11]. For the case of short-lived cosmogenic nuclides ( $^{22}\text{Na}$ ,  $^{57}\text{Co}$ ,  $^{58}\text{Co}$ ,  $^{60}\text{Co}$  and  $^{54}\text{Mn}$ ), for which activity in particular time is strongly dependent on dynamical changes of GCR flux due to solar activity variations we have used approach described in previous section.

The Chelyabinsk-like object modelled in our calculation is LL5 ordinary chondrite with measured composition of major elements (and some additional important trace elements [9]) and known average density  $3.2 \text{ g.cm}^{-3}$  [9]. Modelled object with radius of 9 m was divided into concentric shells with defined thickness, in which fluxes of protons and neutrons were calculated. Having calculated those fluxes and concentrations of target nuclei we used database of available cross sections to obtain final production rates and activities. Our calculations are compared with experimental data. Results of comparison are shown on figure 4.

In the case of the Košice meteorite; the modelled object was a H5 ordinary chondrite with known composition of major elements (and some important trace elements [13]) and known average density of  $3.4 \text{ g.cm}^{-3}$ . Unlike in the case of the Chelyabinsk meteorite calculated activities of cosmogenic radionuclides can be used to estimate preatmospheric size of the meteorite. The modelled objects had radii of 40, 45, 55 and 62.5 cm and were divided into concentric shells with defined thickness, for which fluxes of protons and neutrons were calculated. Having calculated fluxes and concentrations of target nuclei we used database of available cross sections to obtain final production rates and activities. Results of our calculation are compared with experimental data and shown on figures 5,6.

## Results and discussion

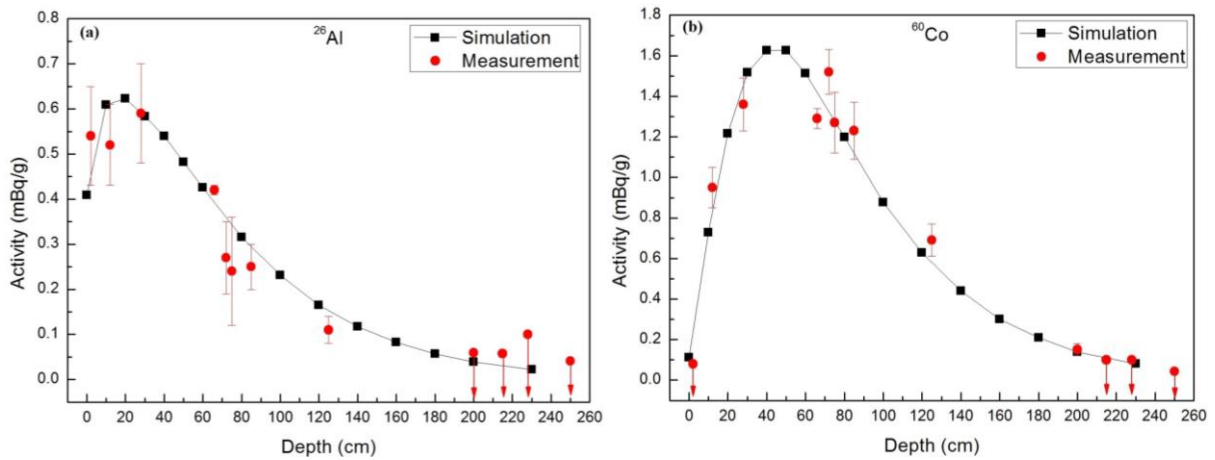


**Figure 9:** Comparison of the simulated depth profiles (black) calculated for distance of the asteroid belt with experimental data assigned to depths (red).

The Chelyabinsk meteorite and its fall were analysed by many modern techniques which provided useful source of information about composition, density, trajectory and size of the meteorite for purpose of our simulations. By using available experimental data we were able to model The Chelyabinsk-like object with radius of 9 m, measured composition density. By Monte-Carlo simulation codes and techniques described in previous sections we have calculated activities and production rates within the modelled object. These results were compared with experimental data (figure 9). Exact depths of samples are unknown. According to our calculation we were able to estimate approximate positions for all measured samples inside of the Chelyabinsk meteorite. The estimation of depths was based on calculated depth profiles, where we assigned position for every sample which was in the best agreement with all simulated depth profiles. As we can see from figure 9 simulated curves and experimental data fit well. The obtained results show relatively small activities. This effect is related to the interaction depth of GCR particles and size of meteorite, where large objects ( $R > 4\text{m}$ ) such as the Chelyabinsk meteorite have exclusively  $2\pi$ -irradiation, which means that incoming GCR particles are not able to induce nuclear reaction in the whole volume of a meteorite.



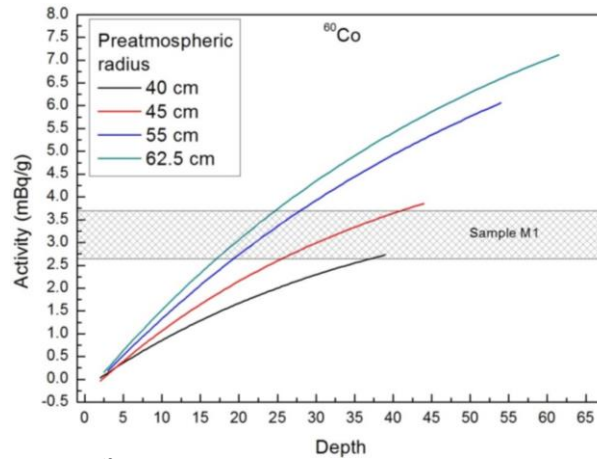


**Figure 10:** Depth profiles of  $^{60}\text{Co}$  for spherical meteoroids with various preatmospheric sizes in comparison with the sample with highest measured activity of  $^{60}\text{Co}$ .

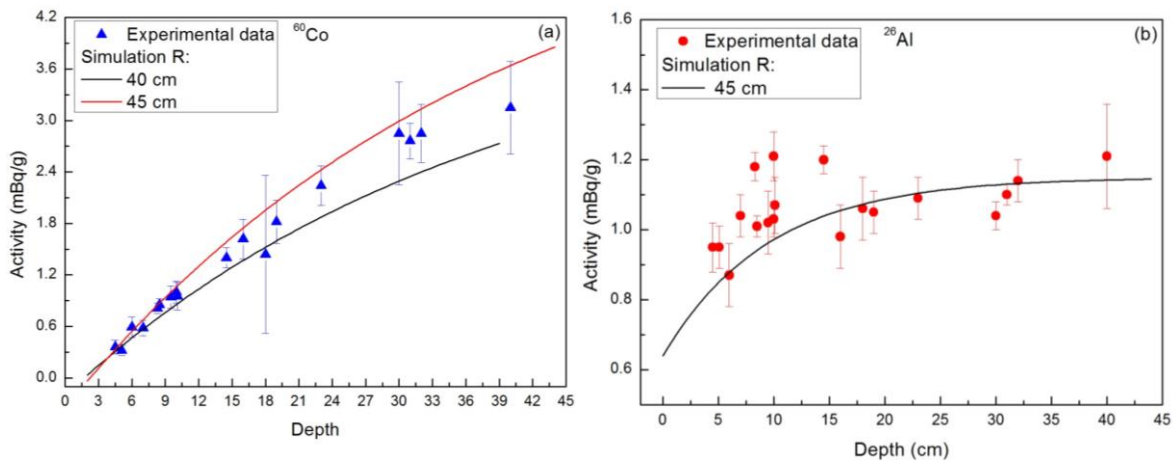


**Figure 11:** Comparison of the simulated depth profiles (black) with experimental data assigned to depths (red).

Using the measured composition and density The Košice-like spherical meteoroids with radii (40, 45, 55, 62.5 cm) were modelled. By using Monte-Carlo simulation codes and techniques described in previous sections we have calculated activities and production rates within the modeled object. The original size estimate of the Košice meteorite was  $R \sim 125$  cm [6] which was based on calculations related to trajectory of the meteoroid body its estimated mass suppose spherical shape of a meteoroid. This kind of estimation can be performed also by using of the calculated activities of cosmogenic radionuclides.  $^{60}\text{Co}$  is the one of the most sensitive depth indicators therefore was applied also in this study [8]. The comparison of simulations for investigated sizes with sample with highest measured activity (M1) is shown on figure 10. The most probable preatmospheric size of the meteorite is between 40 - 45 cm.

Meteorites with smaller sizes would be too small for particle cascade development. This leads to lower activity of  $^{60}\text{Co}$  in the centre of the meteorite and consequently sizes with radii  $< 40$  cm can be excluded from estimation. Meteoroids with radii  $> 45$  cm can't be excluded from our size estimation but from comparison of measurement with simulation (figure 10), no fragment from centre would have been found, which is highly unlikely. This estimation 40-45 cm is in contradiction with estimation based on optical observations (62.5 cm), but still can be reconciled if we consider results from previous chapter (shape effect) that can strongly lower  $^{60}\text{Co}$  activity due to non-spherical shape of the meteoroid (both mentioned size estimates use spherical geometry). The shape effect analysis requires further study of the meteorite fragments for noble gasses ( $^{21}\text{Ne}$ ,  $^{22}\text{Ne}$ ), which provide clues about shielding and locations of the samples within meteoroid body.

We have also estimated approximate position of measured fragments within the meteorite. Results are shown on figure 11. The estimation of depths was based on calculated depth profiles. Determination of position for every sample was based on the requirement of the best agreement of experimental data with all simulated depth profiles. The simulated curves and experimental data fit well.

## **Atmospheric $^{81}\text{Kr}$ as an integrator of cosmic-ray flux over the past 800 kyr**

Long-lived cosmogenic radionuclides carry important information about the past of the terrestrial and space environments. For example, concentrations of  $^{10}\text{Be}$  (half-life = 1.5 Myr) in polar ice and sea sediments reveal the spatial and time variations of the GCR over the past  $10^5$  years [14]. The origin of atmospheric  $^{81}\text{Kr}$  (half-life 229 +/- 11 ky) is also cosmogenic and provide somehow complementary and different perspective from that of  $^{10}\text{Be}$  and  $^{36}\text{Cl}$  on the timescale of  $10^5$  years. The most important difference resides in their transport and residence in the atmosphere.  $^{10}\text{Be}$  is kept in the atmosphere for about a few years and its deposition rate to the archives, affected by GCR distribution and atmospheric transport factors, varies in time and space over the globe by as much as factor of 10 [14]. Understanding of its transport and deposition processes requires robust, sophisticated climate models. In contrast,  $^{81}\text{Kr}$  is a noble-gas nuclide and due its inertness and low solubility in water almost all Kr resides in the atmosphere throughout its lifetime. Only about 2% of the

total terrestrial Kr content is absorbed into the oceans. The  $^{81}\text{Kr}/\text{Kr}$  ratio in the atmosphere is the perfect whole-earth integrator of the GCR flux in the time scale of  $10^5$  years. The measured  $^{81}\text{Kr}/\text{Kr}$  ratio, due to its simplicity, can help verifying models simulating cosmic-ray fluxes and calculating production rates of cosmogenic nuclides.

### **A model for the production rate of $^{81}\text{Kr}$**

The Earth's atmosphere is modelled as a sphere with inner radius of 6378 km and thickness of 100 km. The spherical model is divided into 34 concentric shells of equal thickness ( $30 \text{ g cm}^{-2}$ ) and the average chemical composition, further each shell is divided into 9 latitudinal sections matching to steps of 10 degrees in magnetic latitude. The density and temperature of the modelled atmosphere is approximated by the U.S. Standard Atmosphere [22]. The realistic variation in the density, chemical composition and temperature profile of the atmosphere make negligible effects on the production rate of  $^{81}\text{Kr}$  and other nuclides [15].

The main contribution to cosmogenic nuclide production is done by GCR particles. Fits to lunar experimental data showed that the effective flux of protons and alpha particles with energies above 10 MeV per nucleon at distance of 1 A.U. is  $4.56 \text{ nucleons cm}^{-2} \text{ s}^{-1}$  [16]. This value corresponds to long-term average value of the modulation parameter  $\Phi = 550 \text{ MeV}$  [23].

The geomagnetic field effectively deflects incoming CR particles depending on their angle of incidence and magnetic rigidity, defined as a momentum per charge. For each angle of incidence, there is a critical rigidity below which incoming particles are deflected the way that they cannot reach Earth's atmosphere and induce nuclear reactions. The particle flux is higher around the magnetic poles and lower in the equatorial regions [17].

Records of past magnetic field intensity, dating back to 800 kyr BP, have been obtained from paleomagnetic studies on marine sediments [18]. This most reliable continuous record is used in this calculation, and yields relative paleointensity variations. Guyodo and Valet (1996) calibrated their record with absolute paleointensities obtained from a discontinuous record of lava flows for the past 40 kyr. The mean virtual axis dipole moment (VADM) of the calibrated data of the past 10 kyr, except the one at 2 kyr BP, is very close to the present day VADM of  $8.0 \times 10^{22} \text{ A m}^{-2}$ . By normalizing the 800 kyr VADM data set to its present day value, the record agrees with independent reconstructions of field intensity obtained from other approaches. For this recent period, we adopt the dendrochronologically

derived  $^{14}\text{C}$  record [18] to reconstruct the relative field intensity. This can be done more reliably because major ocean circulation changes can be excluded for the Holocene period.

## Results and discussion

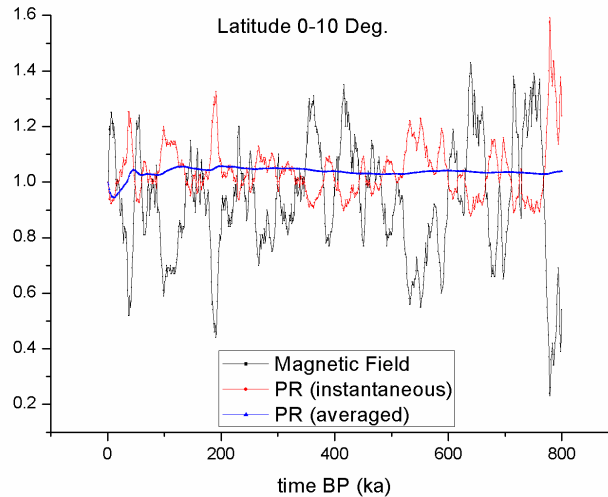


**Figure 12:** The production rates of  $^{81}\text{Kr}$  over time. The black line shows the relative magnetic field intensity in the past 800 kyr adopted in this work. For the past 10 kyr we use the field reconstruction based on the dendrochronologically derived  $^{14}\text{C}$  record [19]; for the period 10-800 kyr, we rely on the reconstruction by [18]. The red line shows the calculated production rate of  $^{81}\text{Kr}$ , normalized to the present-day global average production rate. The blue line is the resulting mean or integrated relative production up to the present.

Results of our calculations are presented in Figure 12. The black line shows the relative magnetic field intensities adopted in this work. The red line represents the corresponding variation of the instantaneous global average production rate of  $^{81}\text{Kr}$  in the Earth's atmosphere. We note that the instantaneous production rate varies less than the magnetic field. The blue line shows the average production rate integrated from present-day to the respective time, a quantity directly relevant to the interpretation of the measured  $^{81}\text{Kr}/\text{Kr}$  ratio. Note that integrated production rate is robust to short-term changes in field intensity, a characteristic that contributes significantly to the advantages of  $^{81}\text{Kr}$  dating.

The statistical uncertainties introduced by the calculations are  $\sim 5\%$ . The systematic uncertainties in the cross sections contribute approximately 10-15%. The standard deviations on the order of 15-20% for their stacked paleomagnetic field records, but short-term variations of such amplitudes around the adopted smoothed field intensity curves have a negligible influence on the integrated production rates of  $^{81}\text{Kr}$ . Therefore, possible systematic

errors in the paleomagnetic records are likely the dominant source of uncertainty for the production rate reported here [18,20]. The systematic uncertainties in our calculated fluxes are difficult to determine, but are probably on the order of 10%. Differences in the calculated and measured neutron fluxes lead to the difference in production rates of investigated nuclides on the level 5-13%. Taking into account all sources of uncertainties mentioned above, production rate of  $^{81}\text{Kr}$  corresponding to present geomagnetic field intensity and long term average solar activity is  $(1.34 \pm 0.10) \times 10^{-6} \text{ atoms cm}^{-2} \text{ s}^{-1}$ . After correcting this value for geomagnetic field variations during the last 800 ky, the averaged production rate is  $(1.39 \pm 0.15) \times 10^{-6} \text{ atoms cm}^{-2} \text{ s}^{-1}$ . As during last 10 thousand years average geomagnetic field was higher than present, the global average production rate is decreased in comparison of present to value  $(1.27 \pm 0.1) \times 10^{-6} \text{ atoms cm}^{-2} \text{ s}^{-1}$ . The production rate of  $^{81}\text{Kr}$  derived from multiple independent measurements was determined to be  $(1.2 \pm 0.1) \times 10^{-6}$  [21], which is in good agreement with our results.

## Summary

This work was dedicated to the Monte-Carlo modelling of cosmic ray interactions with extra-terrestrial and terrestrial matter. We discuss results achieved using calculation models oriented on production of cosmogenic radionuclides commonly used in applied nuclear physics.

We have investigation effects of pre-atmospheric shape on cosmogenic nuclide production. The explanation of effects observed results lies in distance which is required for particle cascade development and number of particles escaping from meteoroid's body. In general flattening of a particular geometry in comparison to sphere renders interior of the meteorite more accessible by particles of higher energy while reduce effective distance for particle cascade development which leads to the leakage of particles of lower energies. The importance of described effects might have different demonstration in geometries with various masses (volumes) in which additional effects related to the size of investigated bodies apply. We have also investigated production rates of cosmogenic radionuclides in The Peekskill meteorite. The results of simulations show sufficient accuracy of calculation for all calculated radionuclides ( $^{10}\text{Be}$ ,  $^{26}\text{Al}$  and  $^{60}\text{Co}$ ).

We have designed a simple calculation model of short-lived radionuclides which allowed us to reconstruct production rates and activities of cosmogenic radionuclides for known meteorite falls. The comparison of relative changes in activity in the solar minimum and maximum shows increasing tendency in variation with decreasing half-life from about 14 % for  $^{60}\text{Co}$  (5.27 y) to ~70 % for  $^{58}\text{Co}$  (70.86 d). Those effects are due to aggregation and decay of radionuclides through the longer period of time. Radionuclides with longer half-lives are less sensitive on changes in GCR flux and their response to change is weaker and slightly delayed. The variation in activity of a radionuclide is also naturally higher near surface, where many lower energetic particles contribute to production and decreases with depth.

Using available experimental data we were able to model meteoroid bodies for The Chelyabinsk meteorite and The Košice meteorite. These results of calculations were compared with experimental data. According to calculated depth profiles we were able to estimate approximate positions for all measured samples inside of the Chelyabinsk meteorite and The Košice meteorite. Every sample was assigned to depth in order to be in the best agreement with all simulated depth profiles.

For the case of the Košice meteorite we have also modelled multiple spherical meteoroids with radii (40, 45, 55, 62.5 cm). The most probable preatmospheric size of the meteorite is between 40 - 45 cm. Meteorites with smaller sizes would not allow full particle cascade development, which leads to lower activity of  $^{60}\text{Co}$  in the centre of the meteorite than are observed. Thus sizes with radii < 40cm can be excluded from estimation. Meteoroids with radii > 45 cm can't be excluded from size estimation but according to measured data in comparison with simulation no fragment from centre would have been found, which is highly unlikely.

Using known records of magnetic field intensity in the past 800 kyr, and designed model of Earth's atmosphere including latitudinal variation of magnetic field we were able to calculate the instantaneous global average production rate of  $^{81}\text{Kr}$  in the Earth's atmosphere up to present day  $(1.39 \pm 0.15) \times 10^{-6} \text{ atoms.cm}^{-2}\text{s}^{-1}$ . Calculated value is in the good agreement with experimental results reached by experimental measurement  $(1.2 \pm 0.1) \times 10^6 \text{ atoms.cm}^{-2}\text{s}^{-1}$ . The measured and calculated  $^{81}\text{Kr}/\text{Kr}$  ratio, due to its simplicity, can help verifying models simulating cosmic-ray fluxes and calculating production rates of cosmogenic nuclides

## Publications

### ADC Vedecké práce zahraničných karentovaných časopisoch

- ADC01** Povinec, Pavel P. - Masarik, Jozef - Sýkora, Ivan - Laubenstein, Matthias - Beňo, Juraj - Kováčik, Andrej - Porubčan, Vladimír: Cosmogenic radionuclides in the Košice meteorite: Experimental investigations and Monte Carlo simulations  
In: Meteoritics & Planetary Science, accepted, (2014)
- ADC02** Povinec, Pavel P. - Laubenstein, Matthias - Jull, A. J. Timothy - Ferrière, Ludovic – Brandstätter, Franz - Sýkora, Ivan - Masarik, Jozef - Beňo, Juraj - Kováčik, Andrej - Koeberl, Christian - Topa, Dan: What do we learn on the meteoroid?  
In: Meteoritics & Planetary Science, under review, (2014)
- ADC03** Masarik, Jozef 50 % - Beňo, Juraj 50 %: Effects of meteoroid shape on cosmogenic nuclide production processes  
In: Meteoritics & Planetary Science, under review, (2014)
- ADC04** Yokochi, R., - Sturchio, N. C., - Purtschert, R., Jiang, - W., Lu, Z. - T., Mueller, P., - Beňo J., - Masarik J  
Atmospheric <sup>81</sup>Kr as an integrator of cosmic-ray flux over the past 800 kyr  
In: Geochimica et Cosmochimica Acta, submitted, (2014)

### AFG Abstrakty príspevkov zo zahraničných vedeckých konferencií

- AFG01** Beňo, Juraj 50 % - Masarik, Jozef 50 %: Effects of meteoroid shape on the production rates of cosmogenic nuclides  
Lit. 5 záz. n.  
In: Meteoritics & Planetary Science. - Vol. 46, Suppl. (2011), s. A19  
[Annual Meeting of the Meteoritical Society 2011. 74th, London, 8.-12.8.2011]
- AFG02** Masarik, Jozef 17% - Porubčan, Vladimír 17% - Beňo, Juraj 17% - Sýkora, Ivan 17% - Povinec, Pavel P. 16% - Tóth, Juraj 16%: Košice meteorite  
Lit. 3 záz. n., 1 tab.  
In: Meteoritics & Planetary Science. - Vol. 47, Spec. Issue SI, Suppl. 1 (2012), Art. No. A262, 2 s.  
[Annual Meeting of the Meteoritical-Society 2012. 75th, Cairns, 12.-17.8.2012]
- AFG03** Beňo, Juraj 40% - Masarik, Jozef 40% - Leya, Ingo 20%: Neutron production and fluxes in extra terrestrial objects  
Lit. 5 záz. n.  
In: Meteoritics & Planetary Science. - Vol. 48, Sp. Iss. , Suppl. 1 (2013), s. A56  
[Annual Meeting of the Meteoritical Society 2013. 76th, Edmonton, 29.7.-2.8.2013]
- AFG04** Masarik, Jozef 50% - Beňo, Juraj 50%: Numerical simulations of <sup>81</sup>Kr production rates  
Lit. 6 záz. n.  
In: Meteoritics & Planetary Science. - Vol. 48, Sp. Iss. , Suppl. 1 (2013), s. A57  
[Annual Meeting of the Meteoritical Society 2013. 76th, Edmonton, 29.7.-2.8.2013]
- AFG05** Povinec, Pavel P. 15% - Masarik, Jozef 15% - Sýkora, Ivan 15% - Laubenstein, Matthias 10% - Beňo, Juraj 15% - Kováčik, Andrej 15% - Porubčan, Vladimír 15%: Cosmogenic nuclides in Košice meteorite  
Lit. 5 záz. n.  
In: Meteoritics & Planetary Science. - Vol. 48, Sp. Iss. , Suppl. 1 (2013), s. A288  
[Annual Meeting of the Meteoritical Society 2013. 76th, Edmonton, 29.7.-2.8.2013]

### AFH Abstrakty príspevkov z domácich vedeckých konferencií

AFH01 Beňo, Juraj 100%: Produkty interakcií kozmického žiarenia v mimozemských objektoch

Recenzované

Lit. 3 zázň.

In: Študentská vedecká konferencia FMFI UK, Bratislava 2012 : Zborník príspevkov. - Bratislava : Fakulta matematiky, fyziky a informatiky UK, 2012. - S. 190. - ISBN 978-80-8147-001-0

[Študentská vedecká konferencia FMFI UK 2012. Bratislava, 25.4.2012]

AFH02 Beňo, Juraj 100%: Vplyv modulácie kozmického žiarenia na produkciu krátko žijúcich nuklidov v mimozemských objektoch

Lit. 2 zázň., 1 obr.

In: Študentská vedecká konferencia FMFI UK, Bratislava 2013 : Zborník príspevkov. - Bratislava : Fakulta matematiky, fyziky a informatiky UK, 2013. - S. 64. - ISBN 978-80-8147-009-7

[Študentská vedecká konferencia FMFI UK 2013. Bratislava, 23.4.2013]